

Supporting Information

Polymorphism and Psuedopolymorphism of an Aromatic Amide: Spontaneous Resolution and Crystal to Crystal Phase Transition

Takako Kato, Iwao Okamoto, Hyuma Masu, Kosuke Katagiri, Masahide Tominaga[†] Kentaro Yamaguchi, Hiroyuki Kagechika and Isao Azumaya

Contents

X-ray Crystallographic Analysis. -----	2
Intermolecular C–H···F interactions. -----	9
DSC analysis for Form I–VII, X and XIII. -----	10

X-ray Crystallographic Analysis.

Crystal data for 1 (Form I). $C_{22}H_{18}F_2N_2O_2$; $M_r = 380.38$ g mol⁻¹, colorless prism measuring 0.40 × 0.40 × 0.40 mm, orthorhombic, $Aba2$, $a = 13.82(2)$, $b = 15.56(1)$, $c = 8.99(1)$ Å, $V = 1932(4)$ Å³, $Z = 4$, $D_c = 1.458$ Mg m⁻³, $T = 298$ K, $\mu = 0.098$ mm⁻¹, $2\theta_{\max} = 54.44^\circ$, 4541 reflections, 1610 unique ($R_{\text{int}} = 0.0144$), $R_1 = 0.0319$, $wR_2 = 0.1060$ (all data) $R_1 = 0.0294$, $wR_2 = 0.1011$ ($I > 2\sigma(I)$) for 129 parameters.

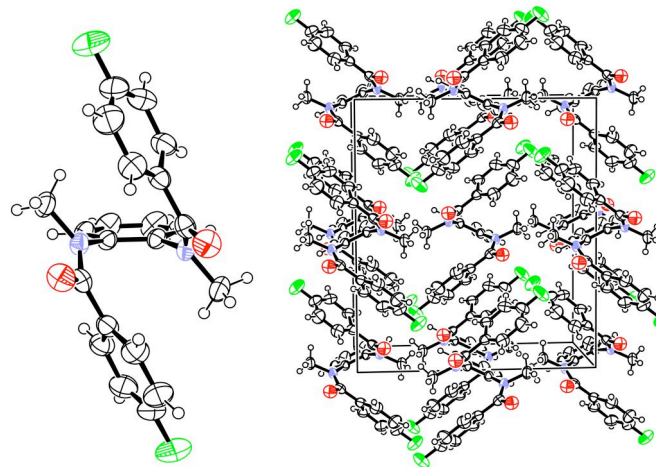


Figure S1. ORTEP diagram of asymmetric unit (left) and packing structure (right) in a crystal of Form I.

Crystal data for 1 (Form II). $C_{22}H_{18}F_2N_2O_2$; $M_r = 380.38$ g mol⁻¹, colorless prism, orthorhombic, $Aba2$, $a = 17.830(2)$, $b = 7.4296(7)$, $c = 13.522(1)$ Å, $V = 1791.2(3)$ Å³, $Z = 4$, $D_c = 1.411$ Mg m⁻³, $T = 90$ K, $\mu = 0.105$ mm⁻¹, $2\theta_{\max} = 56.42^\circ$, 4705 reflections, 1963 unique ($R_{\text{int}} = 0.0185$), $R_1 = 0.0325$, $wR_2 = 0.0558$ (all data) $R_1 = 0.0308$, $wR_2 = 0.0555$ ($I > 2\sigma(I)$) for 128 parameters.

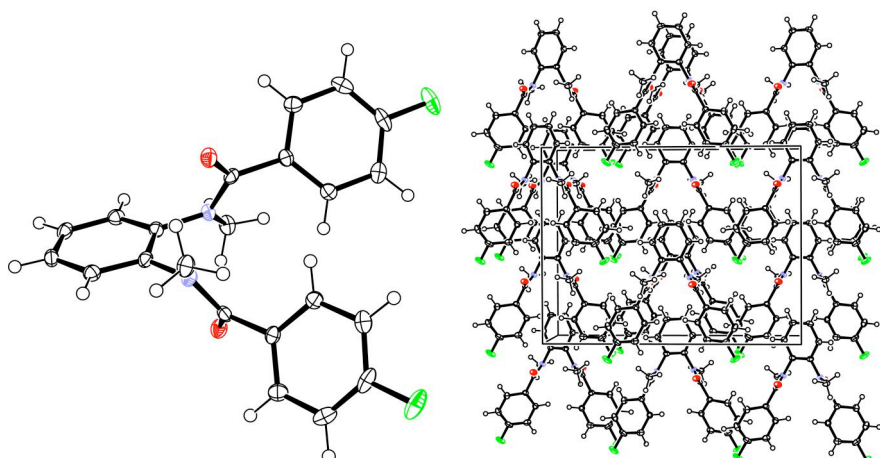


Figure S2. ORTEP diagram of asymmetric unit (left) and packing structure (right) in a crystal of Form II.

Crystal data for 1 (Form III). $C_{22}H_{18}F_2N_2O_2 \cdot 2(\text{CHCl}_3)$; $M_r = 619.12$ g mol⁻¹, colorless prism measuring $0.40 \times 0.40 \times 0.20$ mm, triclinic, $P-1$, $a = 8.905(5)$, $b = 11.135(6)$, $c = 14.695(8)$ Å, $\alpha = 68.790(7)$, $\beta = 88.629(7)$, $\gamma = 87.128(7)$ °, $V = 1357(1)$ Å³, $Z = 2$, $D_c = 1.516$ Mg m⁻³, $T = 150$ K, $\mu = 0.673$ mm⁻¹, $2\theta_{\max} = 56.06$ °, 7024 reflections, 5493 unique ($R_{\text{int}} = 0.0278$), $R_1 = 0.1110$, $wR_2 = 0.3052$ (all data) $R_1 = 0.0955$, $wR_2 = 0.2948$ ($I > 2\sigma(I)$) for 327 parameters.

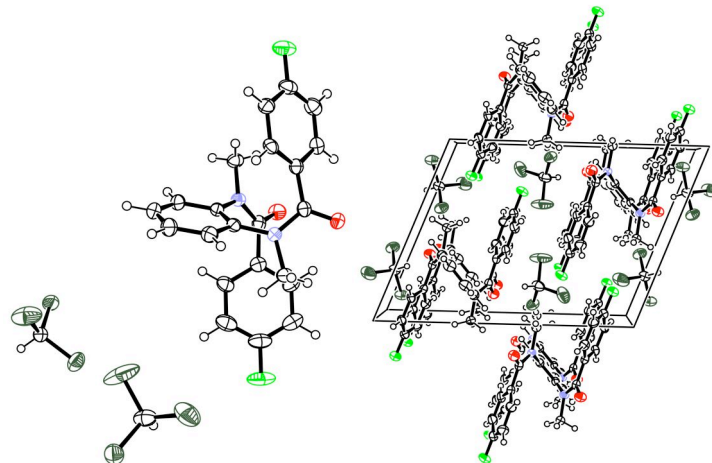


Figure S3. ORTEP diagram of asymmetric unit (left) and packing structure (right) in a crystal of Form III.

Crystal data for 1 (Form IV). $C_{22}H_{18}F_2N_2O_2 \cdot 0.5(\text{CH}_2\text{Cl}_2)$; $M_r = 619.12$ g mol⁻¹, colorless prism measuring $0.40 \times 0.20 \times 0.05$ mm, orthorhombic, $Aba2$, $a = 28.459(3)$, $b = 8.985(1)$, $c = 15.498(2)$ Å, $V = 3963.1(8)$ Å³, $Z = 8$, $D_c = 1.417$ Mg m⁻³, $T = 90$ K, $\mu = 0.233$ mm⁻¹, $2\theta_{\max} = 56.32$ °, 10612 reflections, 3279 unique ($R_{\text{int}} = 0.0503$), $R_1 = 0.0598$, $wR_2 = 0.0952$ (all data) $R_1 = 0.0421$, $wR_2 = 0.0836$ ($I > 2\sigma(I)$) for 269 parameters.

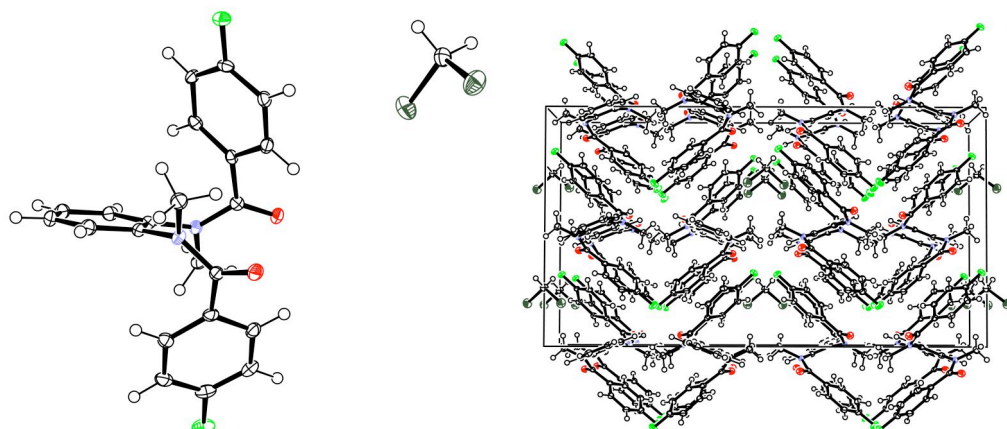


Figure S4. ORTEP diagram of asymmetric unit (left) and packing structure (right) in a crystal of Form IV.

Crystal data for 1 (Form V). $C_{22}H_{18}F_2N_2O_2 \cdot C_3H_6O$; $M_r = 438.46$ g mol⁻¹, colorless prism measuring $0.20 \times 0.10 \times 0.10$ mm, monoclinic, Cc , $a = 10.900(2)$, $b = 14.745(2)$, $c = 13.823(2)$ Å, $\beta = 97.187(2)^\circ$, $V = 2204.1(6)$ Å³, $Z = 4$, $D_c = 1.321$ Mg m⁻³, $T = 120$ K, $\mu = 0.098$ mm⁻¹, $2\theta_{\max} = 54.54^\circ$, 5046 reflections, 3240 unique ($R_{\text{int}} = 0.0253$), $R_1 = 0.0454$, $wR_2 = 0.1087$ (all data) $R_1 = 0.0360$, $wR_2 = 0.1006$ ($I > 2\sigma(I)$) for 293 parameters.

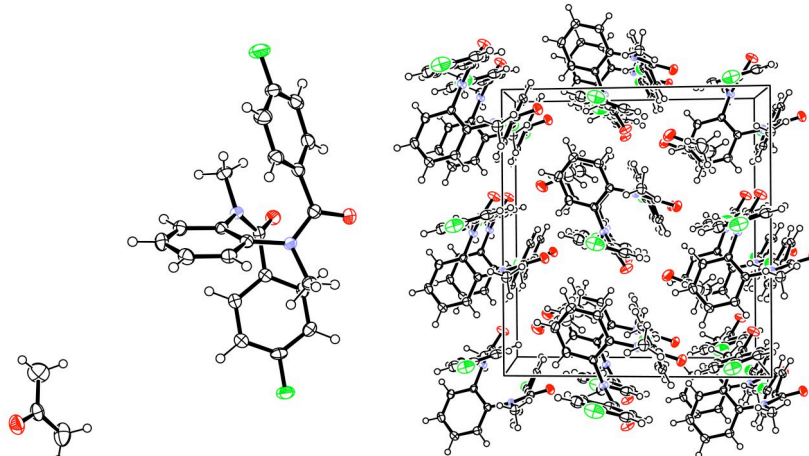


Figure S5. ORTEP diagram of asymmetric unit (left) and packing structure (right) in a crystal of Form V.

Crystal data for 1 (Form VI). $C_{22}H_{18}F_2N_2O_2 \cdot C_4H_8O$; $M_r = 452.49$ g mol⁻¹, colorless prism measuring $0.40 \times 0.30 \times 0.20$ mm, monoclinic, Pn , $a = 9.038(2)$, $b = 10.645(3)$, $c = 11.762(3)$ Å, $\beta = 91.078(3)^\circ$, $V = 1131.5(5)$ Å³, $Z = 2$, $D_c = 1.328$ Mg m⁻³, $T = 120$ K, $\mu = 0.098$ mm⁻¹, $2\theta_{\max} = 51.68^\circ$, 5113 reflections, 3576 unique ($R_{\text{int}} = 0.0203$), $R_1 = 0.0558$, $wR_2 = 0.0653$ (all data) $R_1 = 0.0423$, $wR_2 = 0.0630$ ($I > 2\sigma(I)$) for 300 parameters.

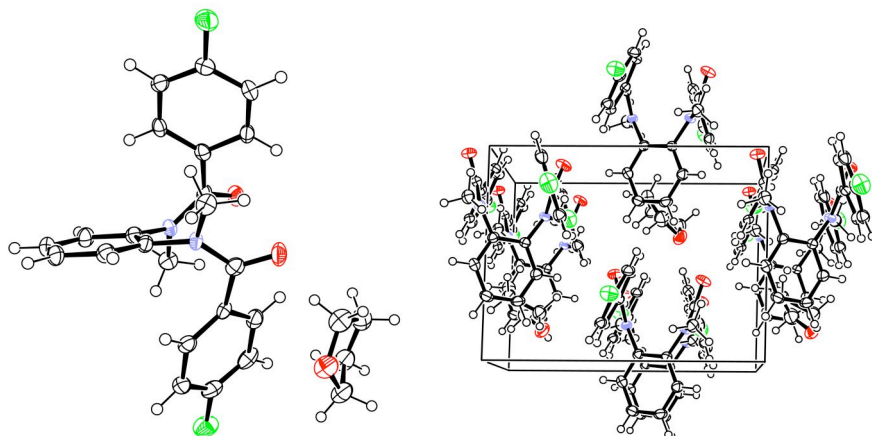


Figure S6. ORTEP diagram of asymmetric unit (left) and packing structure (right) in a crystal of Form VI.

Crystal data for 1 (Form VII). $C_{22}H_{18}F_2N_2O_2 \cdot C_4H_8O_2$; $M_r = 468.49$ g mol⁻¹, colorless prism measuring $0.20 \times 0.20 \times 0.10$ mm, monoclinic, $C2/c$, $a = 12.763(2)$, $b = 9.163(2)$, $c = 20.309(5)$ Å, $\beta = 103.286(3)^\circ$, $V = 2311.5(8)$ Å³, $Z = 4$, $D_c = 1.346$ Mg m⁻³, $T = 90$ K, $\mu = 0.102$ mm⁻¹, $2\theta_{\max} = 54.64^\circ$, 4522 reflections, 2278 unique ($R_{\text{int}} = 0.0880$), $R_1 = 0.0772$, $wR_2 = 0.1694$ (all data) $R_1 = 0.0450$, $wR_2 = 0.1223$ ($I > 2\sigma(I)$) for 156 parameters.

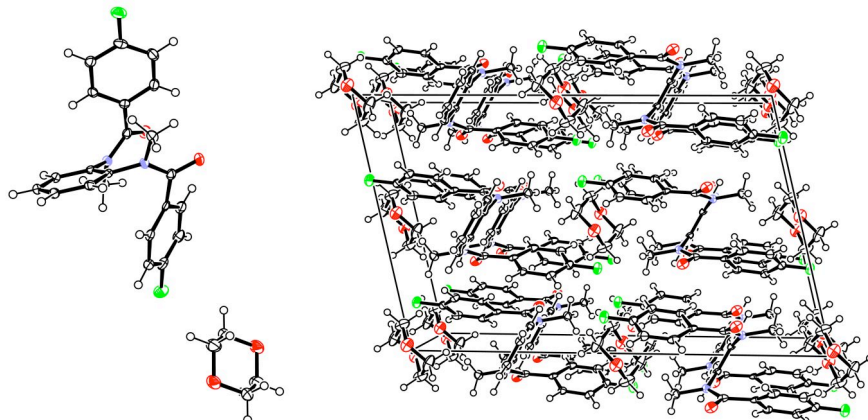


Figure S7. ORTEP diagram of asymmetric unit (left) and packing structure (right) in a crystal of Form VII.

Crystal data for 1 (Form VIII). $C_{22}H_{18}F_2N_2O_2 \cdot C_6H_6$; $M_r = 458.49$ g mol⁻¹, colorless prism measuring $0.20 \times 0.10 \times 0.10$ mm, monoclinic, $C2/c$, $a = 12.804(1)$, $b = 8.9673(8)$, $c = 21.308(2)$ Å, $\beta = 104.445(1)^\circ$, $V = 2369.2(4)$ Å³, $Z = 4$, $D_c = 1.285$ Mg m⁻³, $T = 120$ K, $\mu = 0.092$ mm⁻¹, $2\theta_{\max} = 52.50^\circ$, 5618 reflections, 2339 unique ($R_{\text{int}} = 0.0232$), $R_1 = 0.0567$, $wR_2 = 0.0923$ (all data) $R_1 = 0.0385$, $wR_2 = 0.0845$ ($I > 2\sigma(I)$) for 155 parameters.

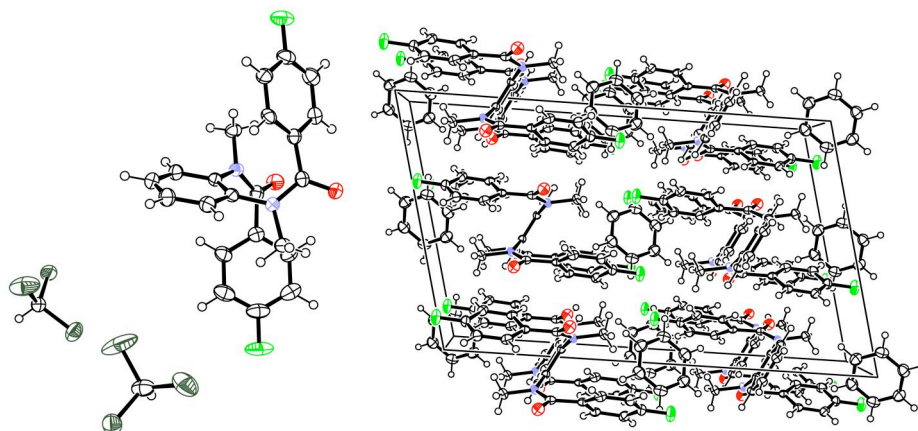


Figure S8. ORTEP diagram of asymmetric unit (left) and packing structure (right) in a crystal of Form VIII.

Crystal data for 1 (Form IX). $C_{22}H_{18}F_2N_2O_2 \cdot C_3H_6O_3$; $M_r = 470.46$ g mol⁻¹, colorless prism measuring $0.20 \times 0.20 \times 0.20$ mm, monoclinic, $C2/c$, $a = 15.585(1)$, $b = 9.0737(7)$, $c = 16.639(1)$ Å, $\beta = 104.404(1)^\circ$, $V = 2279.0(3)$ Å³, $Z = 4$, $D_c = 1.371$ Mg m⁻³, $T = 120$ K, $\mu = 0.107$ mm⁻¹, $2\theta_{\max} = 53.90^\circ$, 5427 reflections, 2299 unique ($R_{\text{int}} = 0.0179$), $R_1 = 0.0478$, $wR_2 = 0.1061$ (all data) $R_1 = 0.0394$, $wR_2 = 0.0997$ ($I > 2\sigma(I)$) for 183 parameters.

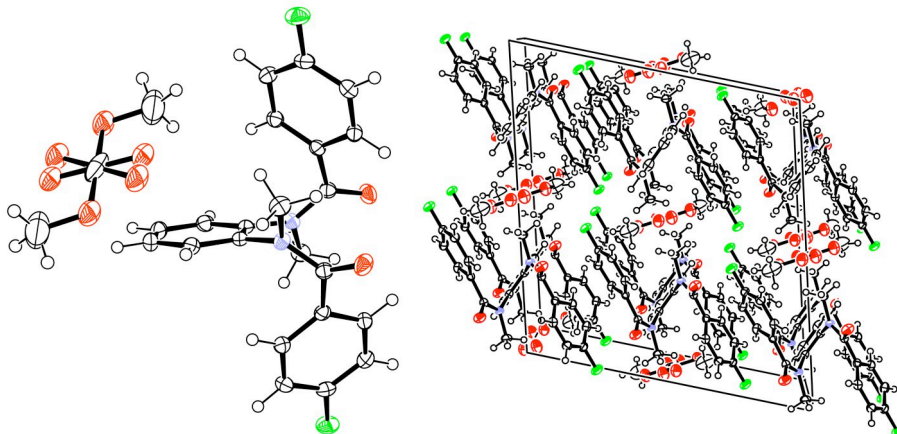


Figure S9. ORTEP diagram of asymmetric unit (left) and packing structure (right) in a crystal of Form IX.

Crystal data for 1 (Form X). $C_{22}H_{18}F_2N_2O_2 \cdot C_4H_8O_2$; $M_r = 468.50$ g mol⁻¹, colorless prism measuring $0.40 \times 0.40 \times 0.10$ mm, trigonal, $P3_1$, $a = b = 9.0756(5)$, $c = 24.324(2)$ Å, $V = 1735.1(2)$ Å³, $Z = 3$, $D_c = 1.345$ Mg m⁻³, $T = 298$ K, $\mu = 0.851$ mm⁻¹, $2\theta_{\max} = 135.60^\circ$, 4995 reflections, 4104 unique ($R_{\text{int}} = 0.039$), $R_1 = 0.0545$, $wR_2 = 0.1496$, $R_1 = 0.0534$, $wR_2 = 0.1479$ ($I > 2\sigma(I)$) for 309 parameters. Flack parameter = 0.1 (2).

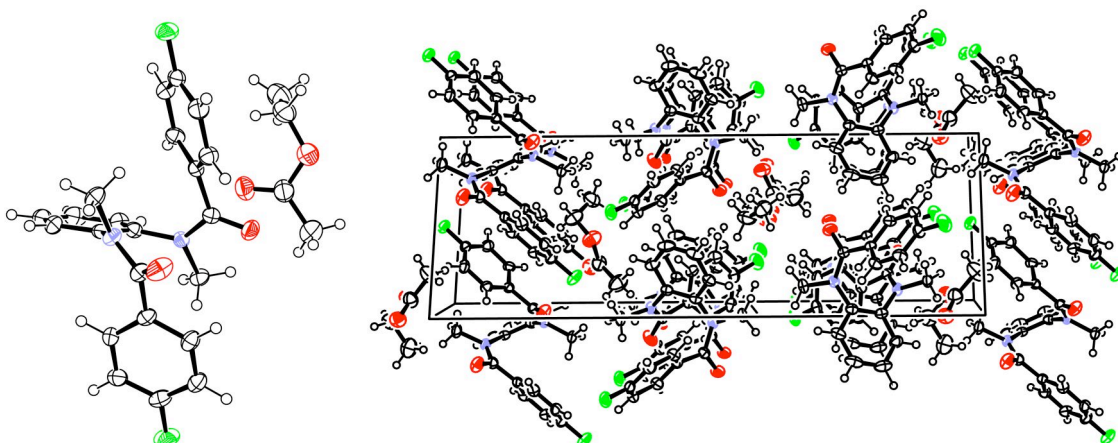


Figure S10. ORTEP diagram of asymmetric unit (left) and packing structure (right) in a crystal of Form X.

Crystal data for 1 (Form XI). $C_{22}H_{18}F_2N_2O_2 \cdot C_4H_8O_2$; $M_r = 468.49$ g mol⁻¹, colorless prism measuring $0.20 \times 0.10 \times 0.10$ mm, trigonal, $P3_2$, $a = b = 9.0311(4)$, $c = 24.502(3)$ Å, $V = 1730.7(2)$ Å³, $Z = 3$, $D_c = 1.349$ Mg m⁻³, $T = 150$ K, $\mu = 0.851$ mm⁻¹, $2\theta_{\max} = 53.92^\circ$, 8575 reflections, 4475 unique ($R_{\text{int}} = 0.0261$), $R_1 = 0.0593$, $wR_2 = 0.1152$ (all data) $R_1 = 0.0460$, $wR_2 = 0.1058$ ($I > 2\sigma(I)$) for 311 parameters. Flack parameter = 0.2(8) (indeterminate).

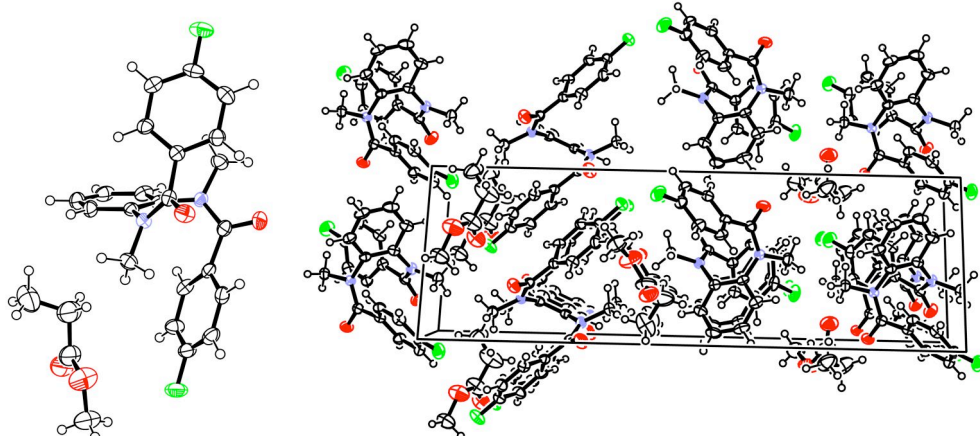


Figure 11. ORTEP diagram of asymmetric unit (left) and packing structure (right) in a crystal of Form XI.

Crystal data for 1 (Form XII). $C_{22}H_{18}F_2N_2O_2 \cdot C_4H_8O_2$; $M_r = 466.47$ g mol⁻¹, colorless prism measuring $0.60 \times 0.40 \times 0.40$ mm, trigonal, $P3_2$, $a = b = 8.9987(3)$, $c = 24.529(2)$ Å, $V = 1720.2(2)$ Å³, $Z = 3$, $D_c = 1.351$ Mg m⁻³, $T = 150$ K, $\mu = 0.102$ mm⁻¹, $2\theta_{\max} = 54.28^\circ$, 8482 reflections, 3941 unique ($R_{\text{int}} = 0.0175$), $R_1 = 0.0447$, $wR_2 = 0.1165$ (all data) $R_1 = 0.0427$, $wR_2 = 0.1153$ ($I > 2\sigma(I)$) for 310 parameters. Flack parameter = -0.3(7) (indeterminate).

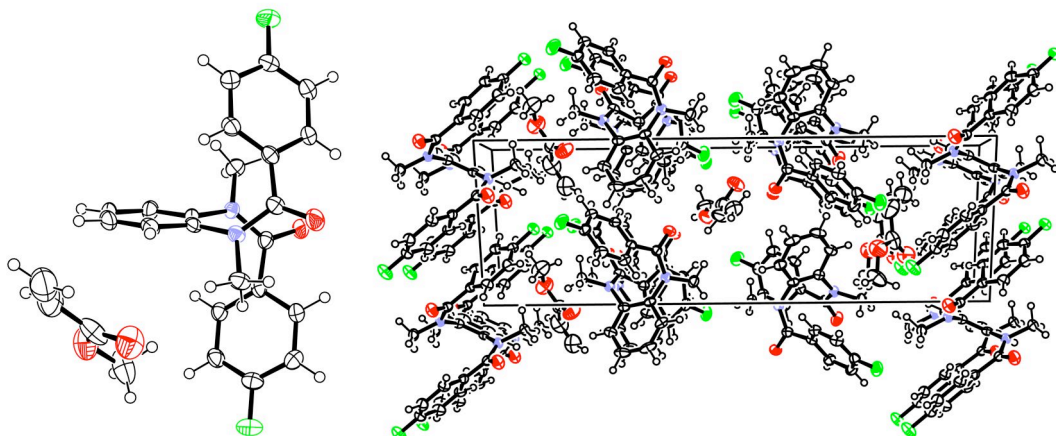


Figure S12. ORTEP diagram of asymmetric unit (left) and packing structure (right) in a crystal of Form XII.

Crystal data for 1 (Form XIII). $C_{22}H_{18}F_2N_2O_2 \cdot C_7H_8$; $M_r = 472.51$ g mol⁻¹, colorless prism measuring $0.10 \times 0.10 \times 0.02$ mm, monoclinic, $C2/c$, $a = 22.531(5)$, $b = 13.650(3)$, $c = 23.223(5)$ Å, $\beta = 91.193(4)^\circ$, $V = 7141(3)$ Å³, $Z = 12$, $D_c = 1.318$ Mg m⁻³, $T = 90$ K, $\mu = 0.093$ mm⁻¹, $2\theta_{\max} = 55.14^\circ$, 21126 reflections, 8104 unique ($R_{\text{int}} = 0.0725$), $R_1 = 0.2233$, $wR_2 = 0.3805$ (all data) $R_1 = 0.0882$, $wR_2 = 0.3008$ ($I > 2\sigma(I)$) for 518 parameters. 1.5 molecules of **1** and 1.5 molecules of toluene are included in an asymmetric unit of the crystal. The positions of hydrogen atoms included in the toluene molecules were not calculated.

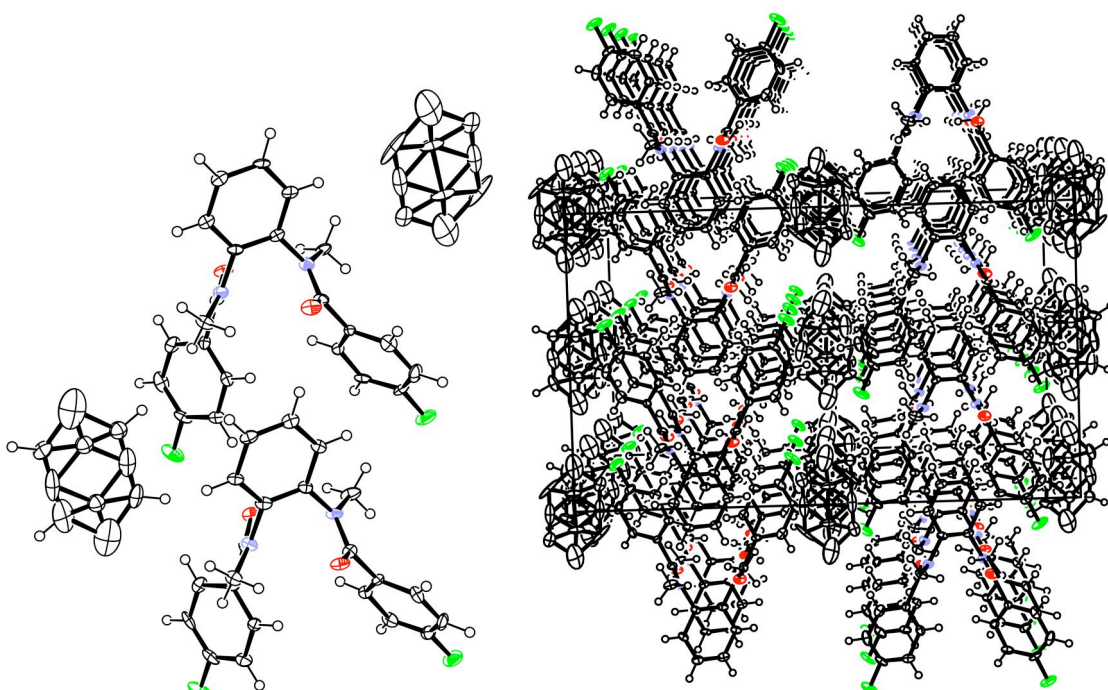


Figure S13. ORTEP diagram of included molecules after treatment of symmetry-expansion (left) and packing structure (right) in a crystal of Form XIII. An asymmetric unit includes 1.5 molecules of **1** and 1.5 molecules of toluene.

Intermolecular C–H···F interactions.

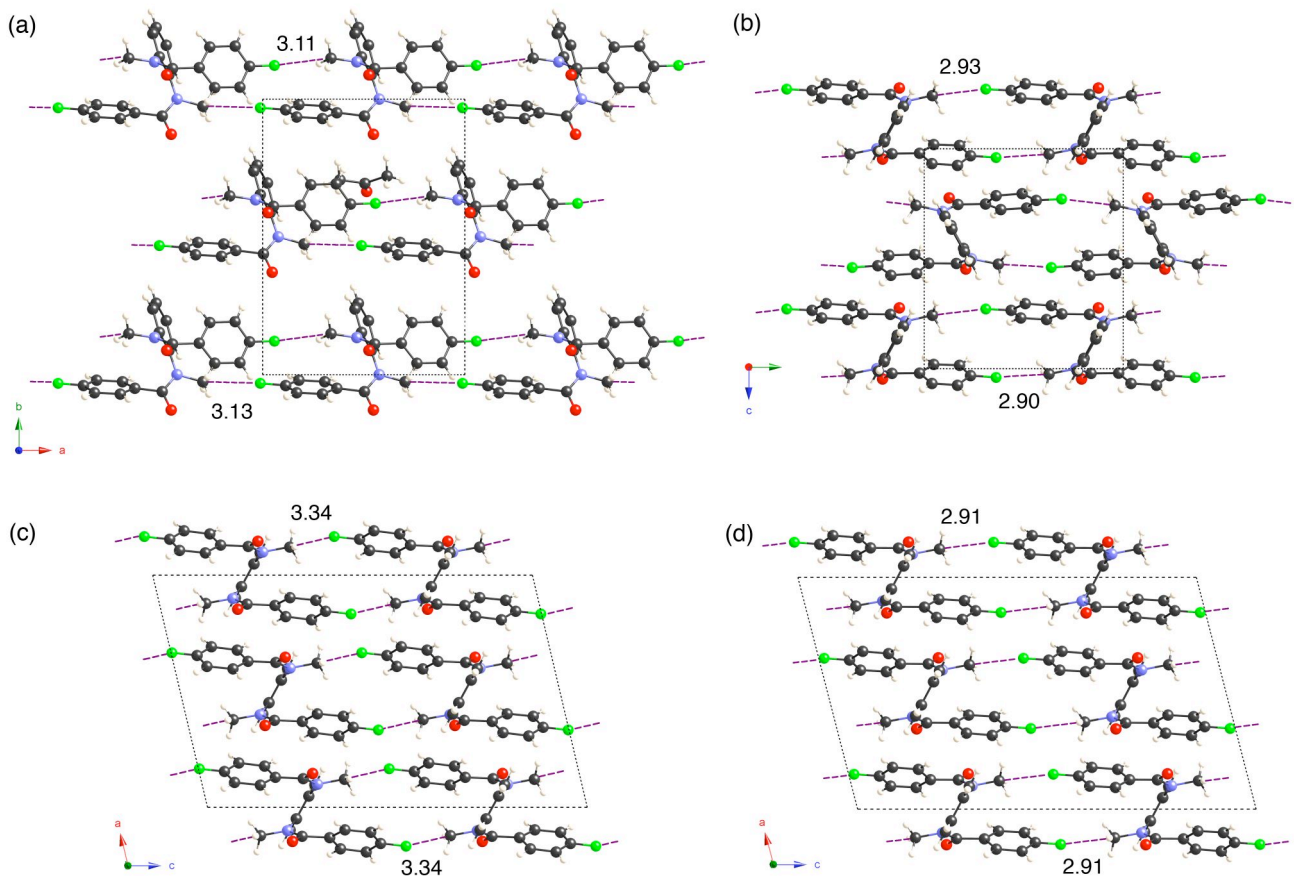


Figure S14. Intermolecular C–H···F interactions in crystals of Form V (a) , VI (b) VII (c) and IIx (d). C–H···F interactions are indicated with purple dot lines. Distances between F and C (methyl) are indicated in Å.

DSC analysis for Form I–VII, X and XIII.

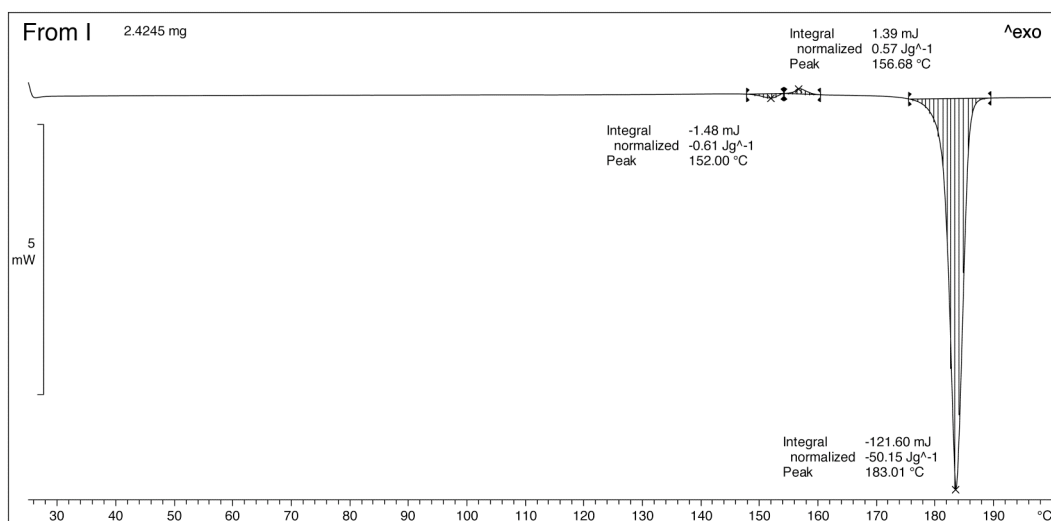


Figure S15. DSC chart of Form I.

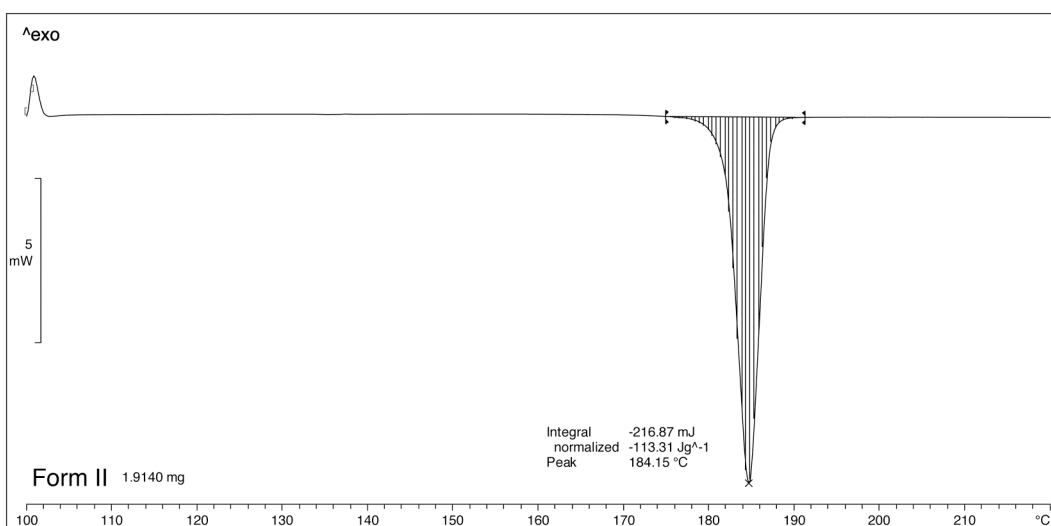


Figure S16. DSC chart of Form II.

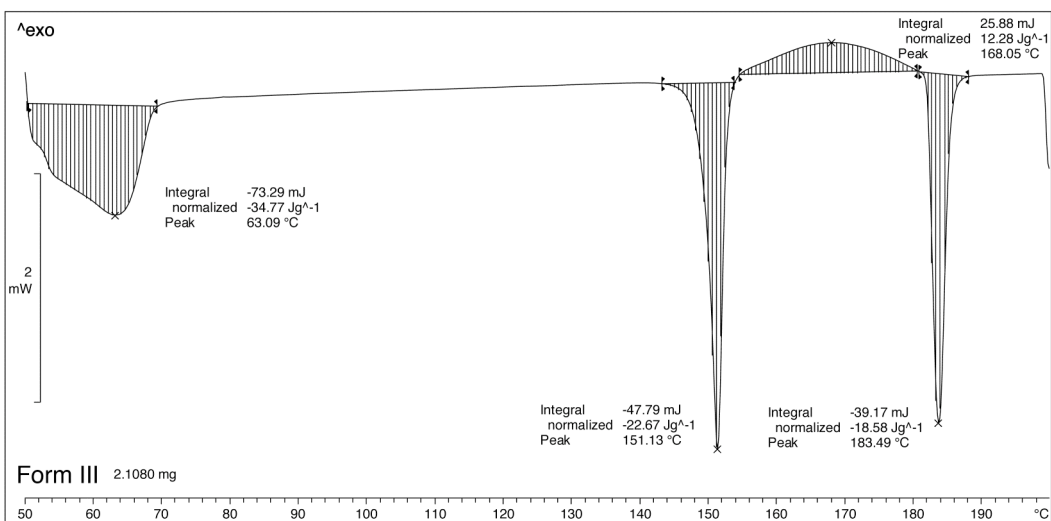


Figure S17. DSC chart of Form III.

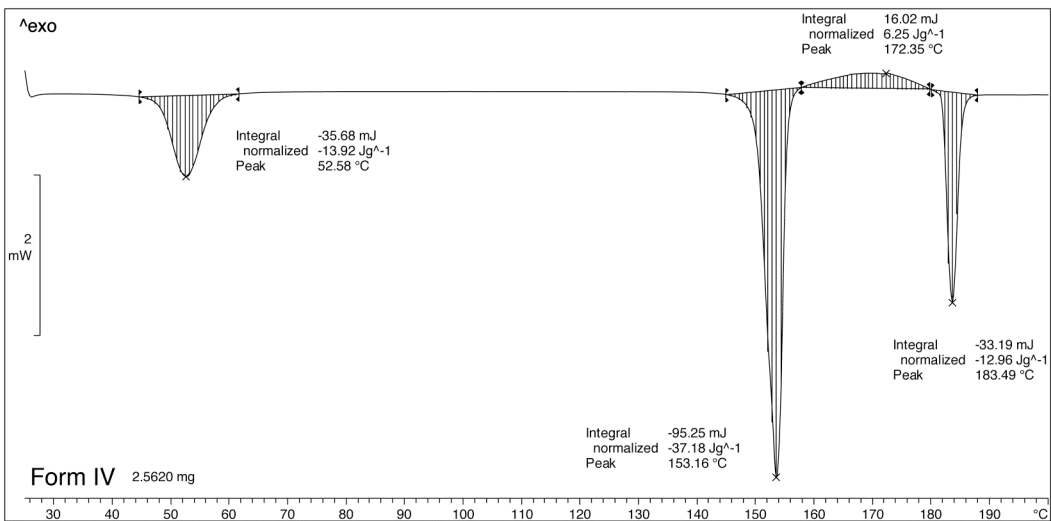


Figure S18. DSC chart of Form IV.

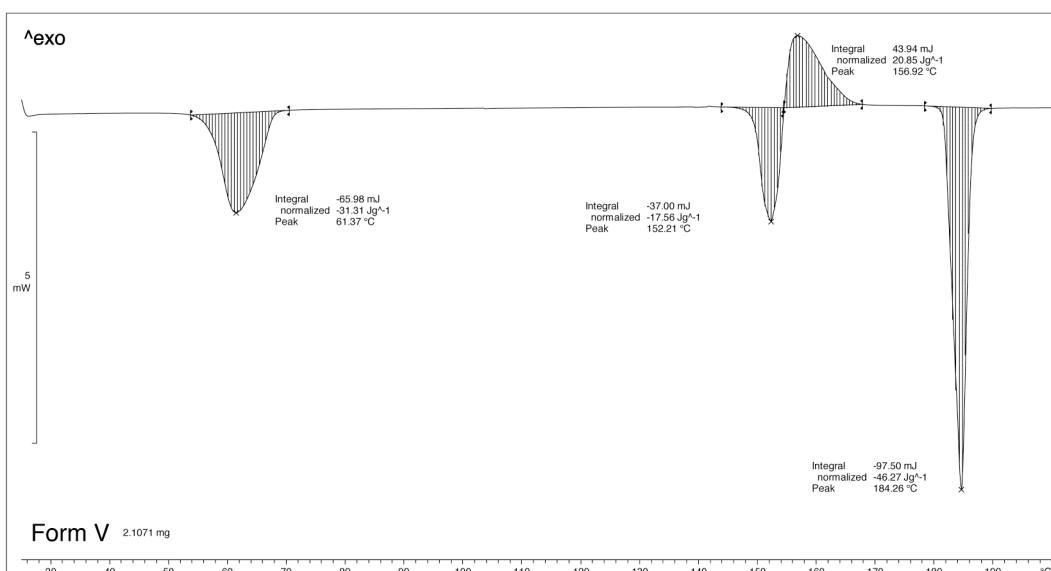


Figure S19. DSC chart of Form V.

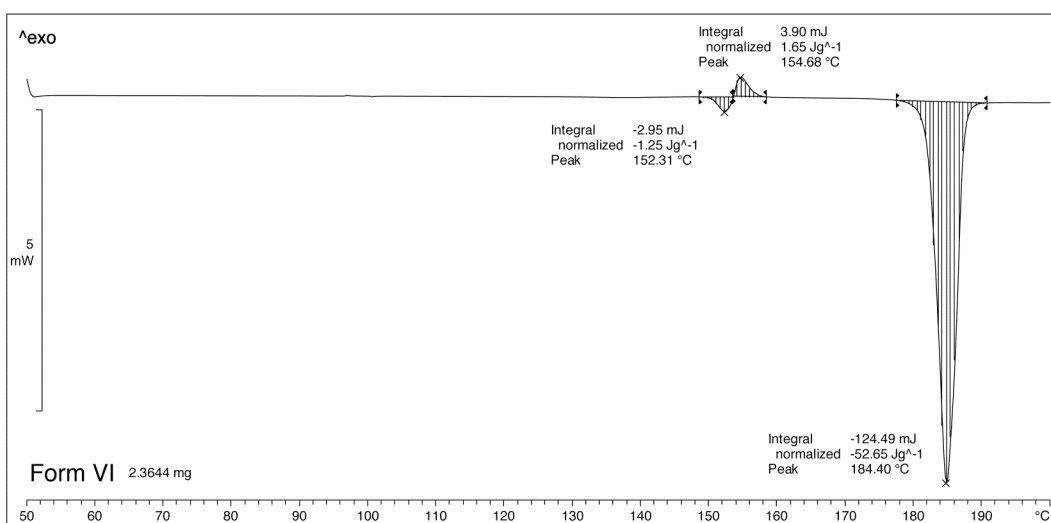


Figure S20. DSC chart of Form VI.

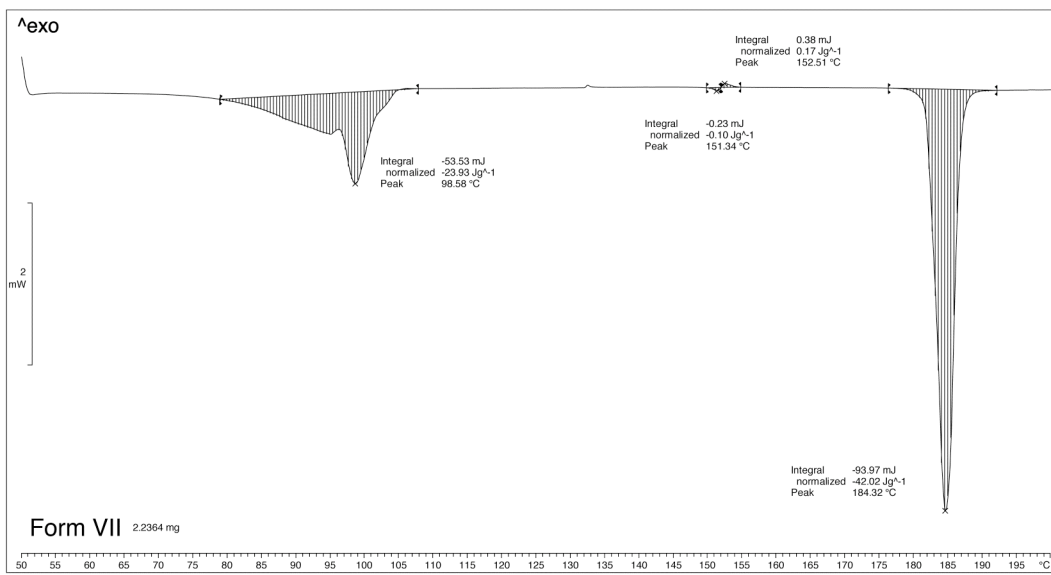


Figure S21. DSC chart of Form VII.

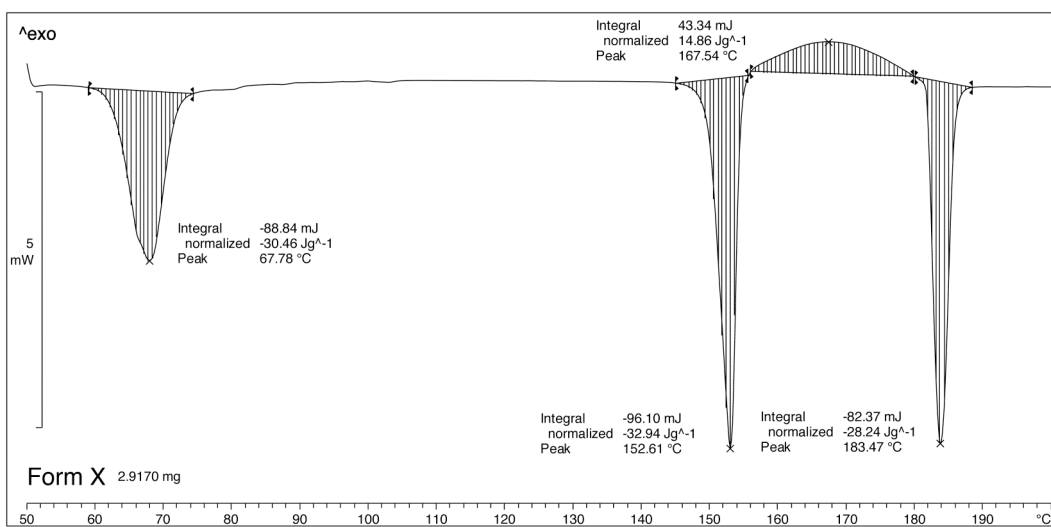


Figure S22. DSC chart of Form X.

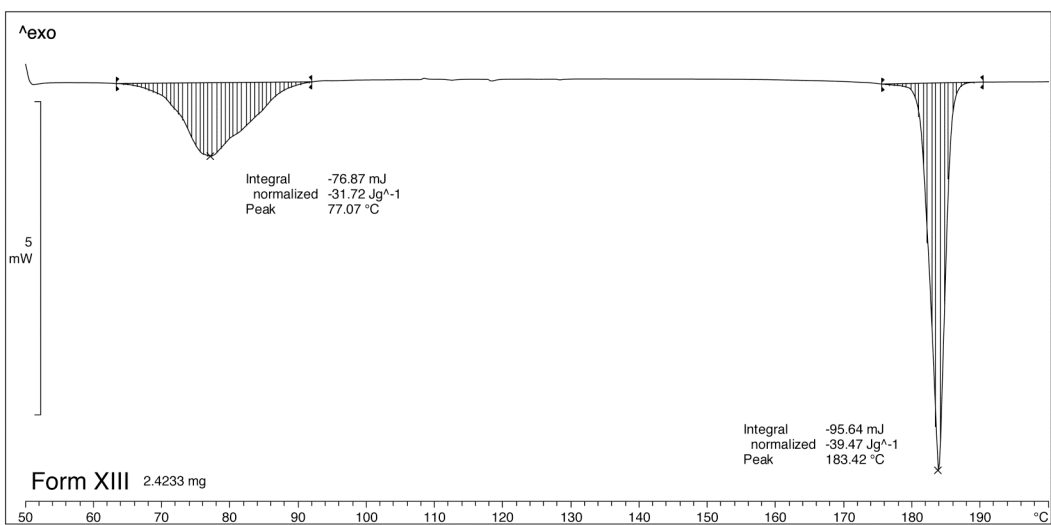


Figure S23. DSC chart of Form XIII.